Inorganic Chemistry

Article

pubs.acs.org/IC

Reversibility in Reactions of Linker-Bridged Distannenes with Terminal Alkynes at Ambient Temperature

Julia Schneider, Jens Henning, Jessica Edrich, Hartmut Schubert, and Lars Wesemann*

Institut für Anorganische Chemie, Universität Tübingen, Auf der Morgenstelle 18, 72076 Tübingen, Germany

Supporting Information

ABSTRACT: The linker-bridged distannene $[(2,6\text{-}Mes_2)\text{-}C_6H_3Sn]_2C_{12}H_8$ (**1**) featuring an acenaphthene linker and the sterically demanding terphenyl substituent Ar^{Me} (= C_6H_3-2,6-Mes_2; Mes = C_6H_2-2,4,6-Me_3) was prepared and characterized by single-crystal analysis, NMR spectroscopy, as well as elemental analysis. Furthermore, the reactivity of distannene **1** and previously reported distannenes **2** and **3**, bearing either a naphthalene or a 9,9-dimethylxanthene backbone and the terphenyl substituent Ar^{Me}, as well as bis(stannylene) **4**, featuring a 9,9-dimethylxanthene backbone and the terphenyl substituent Ar^{iPr} (= C_6H_3-2,6-$Trip_2$; Trip = C_6H_2-2,4,6-*i*-Pr_3), toward terminal alkynes at ambient temperature was investigated, leading to the formal [2 + 2] cycloaddition products **5**–**9**. The reactions of distannene **1** with trimethylsilylacetylene and phenylacetylene, the reaction of distannene **2** with trimethylsilyl–acetylene, as well as the reaction of bis(stannylene) **4** with phenylacetylene show reversibility, while distannenes **2** and **3** react irreversibly with phenylacetylene at room temperature. A van't Hoff analysis of variable-temperature ^{1}H NMR spectra of the cycloadduct of the reaction of distannene **1** with trimethylsilylacetylene afforded a dissociation enthalpy (ΔH_{diss}) of 71.6 kJ·mol^{-1}, which is in surprisingly good agreement with the results of accompanying DFT calculations (ΔH_{diss} = 70.9 kJ·mol^{-1}).

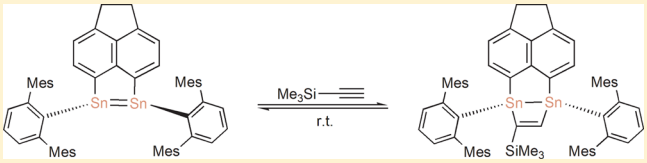

INTRODUCTION

Since the first distannene was structurally characterized in 1976 by Lappert and co-workers,[1] the field of heavy main group compounds with multiple bonds has attracted much attention for almost 40 years and been summarized in various reviews and articles.[2−8] Alkene homologues of the heavier group 14 elements show an increasing deviation from planarity with rising element number and at the same time a decreasing strength of the formal double bond. Hence, especially in the case of R_2SnSnR_2 compounds, the dimers dissociate in solution at ambient temperature. Therefore, with few exceptions the reactivity of monomeric stannylenes is observed instead of the reactivity of the distannene.[2−8]

While the reactivity of disilenes[6,8−11] and digermenes[11−20] with unsaturated organic molecules was studied intensively, similar examples for distannenes are scarce, due to their dissociation disposition in solution. In 1988, Sita and co-worker reported the reaction of an alkyne with Lappert's stannylene $Sn[CH(SiMe_3)]_2$, yielding a stannacyclopropene at −16 °C.[2,21,22] At elevated temperatures the authors observed an equilibrium between the stannacyclopropene, the stannylene, and free alkyne (Scheme 1).

By using the same strained alkyne and reacting it with a monomeric stannylene, Veith et al. synthesized the first 1,2-distannacyclobut-3-ene.[23] As the dimeric form of this stannylene is unknown, the reaction mechanism is proposed to proceed via a formal cheletropic [2 + 1] cycloaddition, followed by an insertion reaction of a second equivalent of the stannylene into a Sn−C bond of the prior formed stannacyclopropene (Scheme 2). In 1990, Sita et al. also reported a 1,2-distannacyclobut-3-ene by reacting Lappert's diorganostannylene with cyclooctyne.[24]

Scheme 1. Reaction of Lappert's Distannene with a Cyclic Alkyne

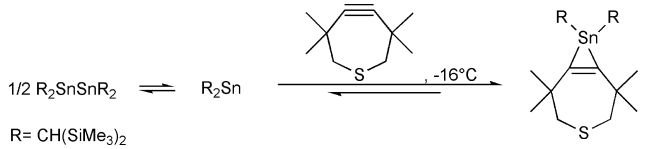

Scheme 2. Synthesis of the First 1,2-Distannacyclobut-3-ene

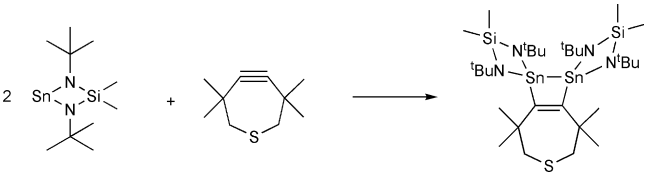

The first reaction of a distannene with a terminal alkyne in a formal [2 + 2] cycloaddition was reported in 1992 by Weidenbruch et al.[25] and used as evidence for the equilibrium of a stannylene and a distannene with the respective cyclotristannane as depicted in Scheme 3. The presence of the stannylene was proven by using 2,3-dimethylbutadiene as trapping reagent.

Received: April 20, 2015
Published: June 1, 2015

ACS Publications © 2015 American Chemical Society

DOI: 10.1021/acs.inorgchem.5b00896
Inorg. Chem. 2015, 54, 6020−6027

Scheme 3. Synthesis of a 1,2-Distannacyclobut-3-ene and a Stannacyclopentene

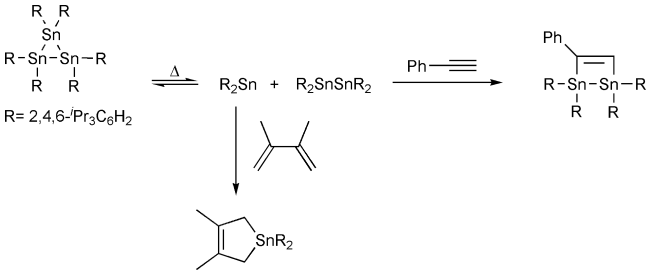

In 2006, the first acyclic distannene which was persistent in solution was synthesized by Lee and co-workers. Reaction of the distannene with phenylacetylene led likewise to the formation of a four-membered cycle as depicted in Scheme 4.[26]

Scheme 4. Reaction of a Persistent Distannene with Phenylacetylene

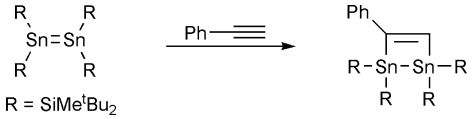

None of these reactions was observed to be reversible except for the reaction of Lappert's stannylene with the thiocycloheptyne (Scheme 1). However, Power et al. reported a reversible cycloaddition of ethylene with distannynes in 2009 (Scheme 5).[27]

Scheme 5. Reversible Reaction of Ethylene with Distannyne

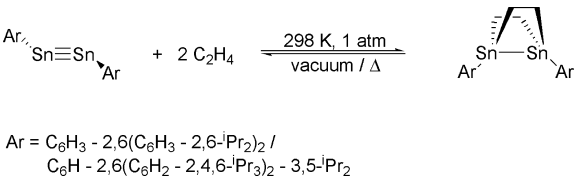

Only recently, to our knowledge, has the first example of a cycloaddition reaction of a digermene with nitriles which shows reversibility at 100 °C been reported.[28]

Previously, we reported the synthesis of linker-bridged distannenes as well as a bis(stannylene) bearing either a naphthalene or a 9,9-dimethylxanthene backbone and the sterically demanding terphenyl substituents Ar^{Me} (= C_6H_3-2,6-Mes_2; Mes = C_6H_2-2,4,6-Me_3)[29] (**2**/**3**) or Ar^{iPr} (= C_6H_3-2,6-$Trip_2$; Trip = C_6H_2-2,4,6-*i*-Pr_3) (**4**) (Figure 1).[30]

Herein, we report the synthesis and structural characterization of a linker-bridged distannene featuring an acenaphthene backbone and the bulky substituent Ar^{Me} (**1**). The investigation of the reactivity of distannenes **1**−**3** and bis(stannylene) **4** toward terminal alkynes showed reversibility at ambient temperature in the cases of distannene **1** with trimethylsilylacetylene or phenylacetylene, distannene **2** with trimethylsilylacetylene, as well as bis(stannylene) **4** with phenylacetylene. However, distannenes **2** and **3** react irreversibly with phenylacetylene at room temperature. The thermodynamic parameters ΔH_{diss} and ΔS_{diss} of the dissociation of cycloaddition product **6** were determined by means of a van't Hoff analysis of variable-temperature ^{1}H NMR spectra.

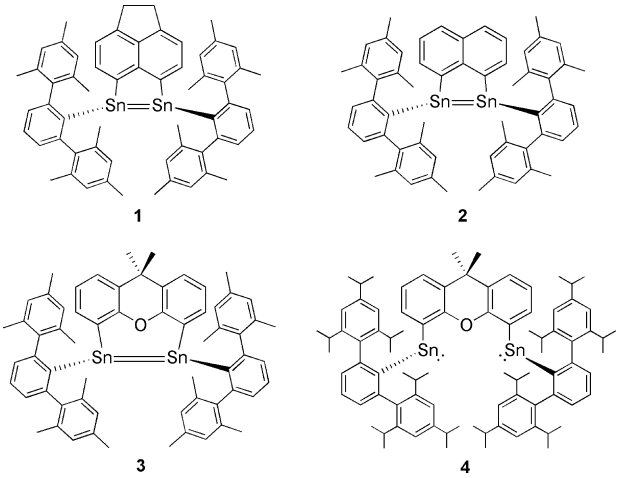

Figure 1. Intramolecular cyclic distannenes **1**−**3** and bis(stannylene) **4**.

Furthermore, quantum chemical calculations were carried out in order to elucidate the reactions of distannene **1** with trimethylsilylacetylene or phenylacetylene as well as the reaction of distannene **2** with phenylacetylene.

RESULTS AND DISCUSSION

Synthesis. Compound **1** is synthesized by reacting 5,6-dilithioacenaphthene, which was prepared from 5,6-dibromoacenaphthene and *n*-butyllithium, and $[Ar^{Me}SnCl]_2$ (Scheme 6).[30,31] The intense green product is highly soluble in

Scheme 6. Synthesis of Distannene 1

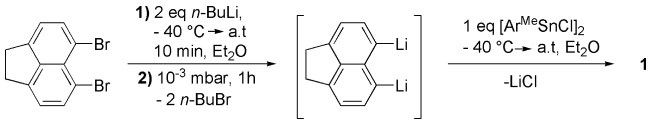

hydrocarbon and ether solvents and can be crystallized from concentrated solutions in *n*-hexane in 52% yield at ambient temperature. Distannene **1** is sensitive toward air and moisture and was characterized by single-crystal analysis, NMR spectroscopy in solution, as well as elemental analysis.

Crystallographic Analysis. Single-crystal analysis reveals a tin−tin distance of 2.7838(2) Å, which is slightly longer than in the case of distannene **2** (2.7299(3) Å).[30] Reported tin−tin distances of distannenes range from 2.668(1) to 3.0009(7) Å; hence, distannene **1** features a rather short tin−tin distance.[2,29,32−39] While the naphthalene backbone of distannene **2** is planar, the acenaphthene backbone of distannene **1** is slightly distorted (central torsions angle C58−C59−C60−C52 = 176.9(0)°). Furthermore, distannene **1** shows a trans-bent structure with bent angles θ = 43° and 65° and a twist angle τ = 65°.

NMR Spectroscopy. While distannene **2** reveals C_2 symmetry in solution NMR spectroscopy and in the solid state structure, distannene **1** shows no C_2 symmetry in the solid state. However, in solution the ^{119}Sn NMR spectrum of **1** exhibits one singlet signal at 375 ppm with satellite signals caused by scalar coupling of $^1J(^{119}Sn,^{117}Sn)$ = 9478 ± 30 Hz, which indicates the chemical equivalence of the two tin atoms. In comparison, distannene **2** shows a quite similar NMR

DOI: 10.1021/acs.inorgchem.5b00896
Inorg. Chem. 2015, 54, 6020−6027

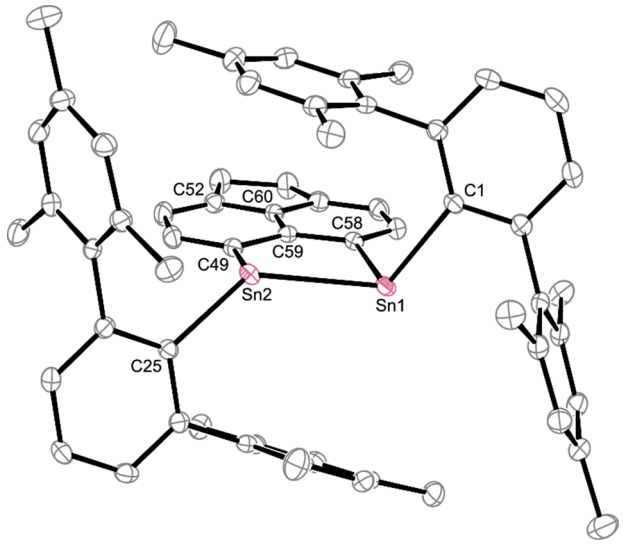

Figure 2. ORTEP plot of the molecular structure of distannene **1**. All hydrogen atoms are omitted; ellipsoids are given at the 50% probability level. Selected interatomic distances [Angstroms] and angles [degrees]: Sn1−Sn2 2.7838(2), Sn1−C1 2.208(2), Sn1−C58 2.202(2), Sn2−C25 2.178(2), Sn2−C49 2.157(2), C49−C58 2.565(2), C58−Sn1−C1 102.11(6), C58−Sn1−Sn2 84.98(4), C1−Sn1−Sn2 114.92(4), C49−Sn2−C25 106.31(6), C49−Sn2−Sn1 88.63(4), C25−Sn2−Sn1 134.69(4), C58−Sn1−Sn2−C49 9.40(6).

spectrum with δ = 396 ppm and $^{1}J(^{119}\mathrm{Sn},^{117}\mathrm{Sn})$ = 9470 ± 30 Hz.

Reactivity Studies. Furthermore, the reactivity of distannenes **1**−**3** as well as bis(stannylene) **4** toward terminal alkynes was studied. In all cases the particular distannene or bis(stannylene) was dissolved in *n*-hexane, and an excess of the alkyne was added at ambient temperature. While in the reactions of distannenes **1** and **3** with the terminal alkynes an off-white or colorless precipitate was formed, reactions of distannene **2** and bis(stannylene) **4** with phenylacetylene lead to a color change from intense green to red-orange and from red-brown to light yellow, respectively. In all reactions the respective 1,2-distannacyclobut-3-enes **5**−**9** (Scheme 7) were obtained. The new four-membered ring compounds **5**−**9** were characterized by single-crystal analysis, elemental analysis, and NMR spectroscopy in solution.

Crystallographic Analysis. Single-crystal analysis shows comparable ring geometries for compounds **5**−**9** in the solid state. Compounds **5**−**8** were crystallized in low to moderate yield (39−68%) from concentrated solutions in benzene or *n*-hexane at room temperature. Pale yellow single crystals of compound **9** were obtained from a concentrated solution in ether at −40 °C. The results of the crystal structure analysis are depicted in Figures 3−7.

Similar trends appear for the four-membered rings **5**−**7** compared to the respective distannenes. First, the Sn−Sn bond lengths are barely different. While distannene **1** exhibits an Sn−Sn bond length of 2.7838(2) Å, for Ar^{Me}AnapPh **5** and Ar^{Me}AnapTMS **6** slightly shortened bonds of 2.7576(2) and 2.7668(3) Å are observed. Distannene **2** possesses a Sn−Sn bond length of 2.7299(3) Å, whereas Ar^{Me}NapPh **7** shows minimal elongation to 2.7444(2) Å. A reason for these small changes can be seen in the rigid acenaphthene or naphthalene backbones. Second, the C−C bond lengths of the 1,2-distannacyclobut-3-enes exhibit a clear elongation compared

Scheme 7. Reactions of Compounds 1−4 with Acetylenes[a]

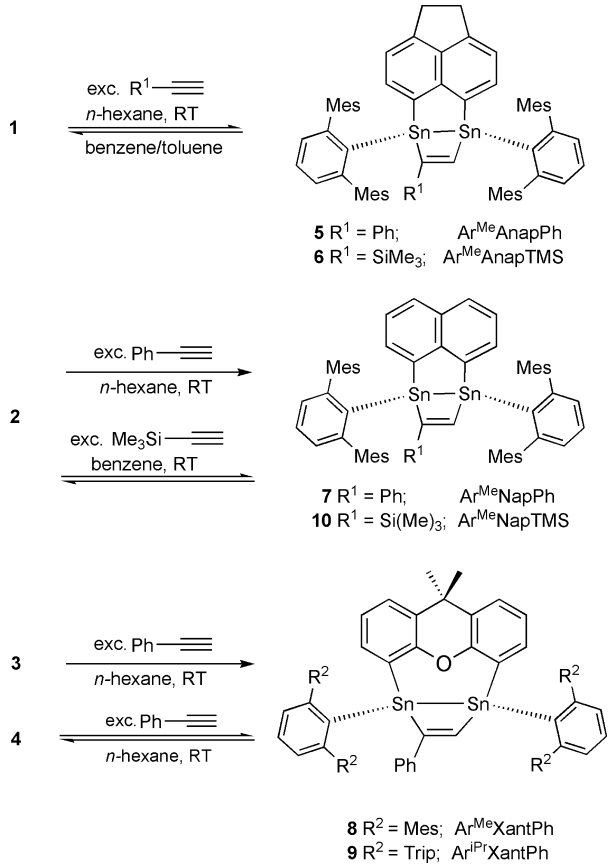

[a]Compound **10** is only characterized by NMR-spectroscopic findings.

to the expected value of a C−C triple bond of around 1.2 Å. Compounds **5**−**7** show C−C bond lengths of 1.34 Å, which indicate a decrease in bond order. Third, a change in geometry is observed. While compounds **1** and **2** show the typical trans bending of distannenes, the geometries of compounds **5**−**7** are converted into a cis bending. This is indicated by both *ipso*-carbon atoms of the Ar^{Me} substituents lying on the same side of the least-squares planes which is defined by the two tin atoms and the *ipso*-carbon atoms of the backbones.

In the case of Ar^{Me}XantPh **8** we observe the same trends in bond lengths as described for compounds **5**−**7**; however, the shortening of the tin−tin distance is with >0.1 Å more pronounced. Ar^{iPr}XantPh **9** reveals with 1.38 Å the strongest shortening of the tin−tin distances, which indicates the remarkable flexibility of the xanthene backbone. As a result, the backbone loses planarity and folding along the O13−C6 axis (folding angle 138°). In comparison, the xanthene backbone of Ar^{Me}XantPh **8** reveals a folding angle of 135°. Further crystallographic details are available in the Supporting Information.

NMR Spectroscopy. For compounds **5**−**8** ^{1}H, ^{13}C, as well as ^{119}Sn NMR spectra are consistent with the molecular symmetries of the solid state structures. In the case of Ar^{iPr}XantPh **9** the assignment of the signals in ^{1}H and ^{13}C NMR spectra was difficult due to the reversibility of the reaction. Nevertheless, it is possible to assign the singlet resonance for the olefinic proton attached to the four-membered ring in the ^{1}H NMR spectrum of each distannacyclobutene. The assignment is unambiguous because

DOI: 10.1021/acs.inorgchem.5b00896
Inorg. Chem. 2015, 54, 6020−6027

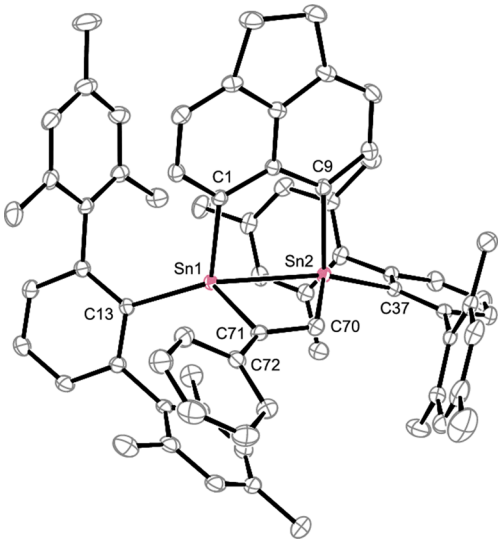

Figure 3. ORTEP plot of the molecular structure of Ar^{Me}AnapPh **5**. All hydrogen atoms and cocrystallized solvent molecules are omitted; ellipsoids are given at the 50% probability level. Selected interatomic distances [Angstroms] and angles [degrees]: Sn1−Sn2 2.75762(1), Sn1−C13 2.1658(1), Sn1−C1 2.1711(1), Sn1−C71 2.1839(1), Sn2−C37 2.1583(1), Sn2−C9 2.1686(1), Sn2−C70 2.169(2), C70−C71 1.342(2), C1−C9 2.582(2), C13−Sn1−C1 117.12(5), C1−Sn1−C71 97.11(5), C13−Sn1−Sn2 147.95(4), C1−Sn1−Sn2 86.85(4), C71−Sn1−Sn2 71.68(4), C37−Sn2−C9 110.29(5), C9−Sn2−C70 103.98(5), C37−Sn2−Sn1 155.27(4), C9−Sn2−Sn1 88.02(4), C70−Sn2−Sn1 70.33(4), C71−C70−Sn2 110.93(10), C70−C71−Sn1 107.00(1).

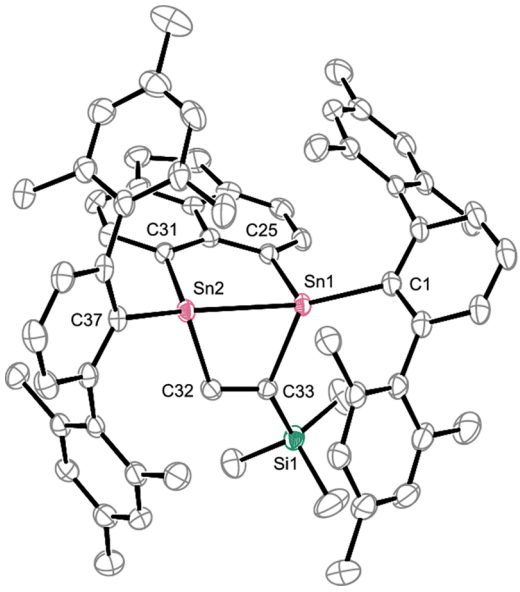

Figure 4. ORTEP plot of the molecular structure of Ar^{Me}AnapTMS **6**. All hydrogen atoms are omitted; ellipsoids are given at the 50% probability level. Selected interatomic distances [Angstroms] and angles [degrees]: Sn1−Sn2 2.7669(2), Sn1−C25 2.177(3), Sn1−C1 2.179(3), Sn1−C33 2.193(3), Sn2−C31 2.156(3), Sn2−C37 2.166(2), Sn2−C32 2.174(3), C32−C33 1.342(4), C31−C25 2.584(4), C25−Sn1−C1 117.74(1), C25−Sn1−C33 98.17(1), C25−Sn1−Sn2 86.20(7), C33−Sn1−Sn2 72.46(7), C31−Sn2−C37 115.72(10), C31−Sn2−C32 101.66(1), C31−Sn2−Sn1 88.80(7), C32−Sn2−Sn1 69.37(7).

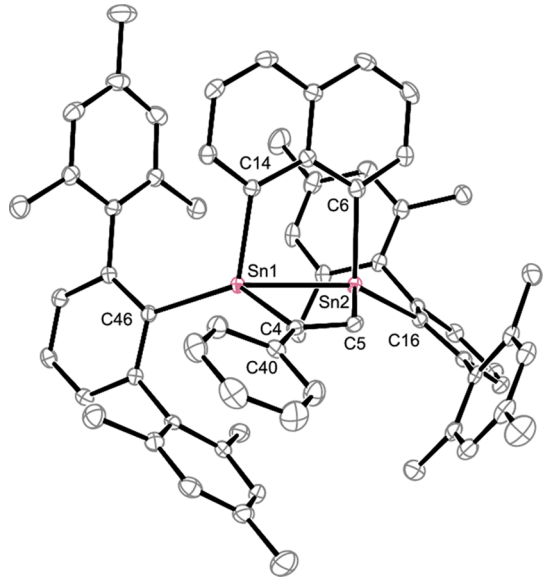

Figure 5. ORTEP plot of the molecular structure of Ar^{Me}NapPh **7**. All hydrogen atoms are omitted; ellipsoids are given at the 50% probability level. Selected interatomic distances [Angstroms] and angles [degrees]: Sn1−Sn2 2.7444(2), Sn1−C46 2.164(2), Sn1−C14 2.177(2), Sn1−C4 2.184(2), Sn2−C16 2.161(2), Sn2−C6 2.162(2), Sn2−C5 2.169(2), C4−C5 1.341(2), C14−C6 2.554(2), C46−Sn1−C14 118.66(6), C46−Sn1−C4 126.73(7), C14−Sn1−C4 99.22(6), C46−Sn1−Sn2 140.40(5), C14−Sn1−Sn2 86.44(5), C4−Sn1−Sn2 71.96(5), C5−Sn2−Sn1 70.36(5), C5−C4−Sn1 106.53(1), C4−C5−Sn2 111.00(1), C16−Sn2−C6 115.53(7), C16−Sn2−C5 116.35(7), C6−Sn2−C5 104.51(7), C16−Sn2−Sn1 150.45(5), C6−Sn2−Sn1 88.16(5), C5−Sn2−Sn1 70.36(5), C5−C4−Sn1 106.53(1), C40−C4−Sn1 127.12(1), C5−C4−C40 125.7(2).

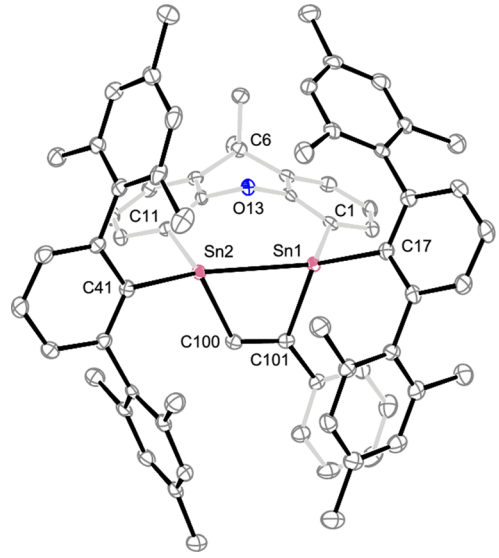

Figure 6. ORTEP plot of the molecular structure of Ar^{Me}XantPh **8**. All hydrogen atoms are omitted; ellipsoids are given at the 50% probability level. Selected interatomic distances [Angstroms] and angles [degrees]: Sn1−Sn2 2.8965(2), Sn1−C101 2.188(2), Sn2−C100 2.159(2), C100−C101 1.337(3), Sn1−C1 2.182(2), Sn1−C17 2.184(2), Sn2−C11 2.185(2), Sn2−C41 2.184(2), Sn1−C101−C100 108.5(2), Sn2−C100−C101 113.3(2), C1−Sn1−C17 103.92(9), C11−Sn2−C41 102.98(9), C1−Sn1−Sn2 108.02(6), C11−Sn2−Sn1 107.94(6), C17−Sn1−Sn2 140.29(6), C41−Sn2−Sn1 147.09(6), C1−Sn1−Sn2−C11 −4.65(9).

DOI: 10.1021/acs.inorgchem.5b00896
Inorg. Chem. 2015, 54, 6020−6027

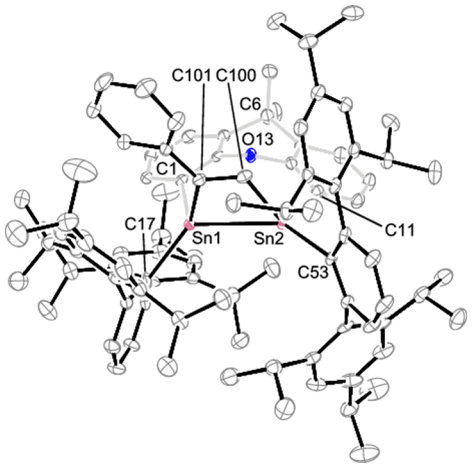

Figure 7. ORTEP plot of the molecular structure of Ar^{iPr}XantPh **9**. All hydrogen atoms are omitted; ellipsoids are given at the 50% probability level. Selected interatomic distances [Angstroms] and angles [degrees]: Sn1−Sn2 2.8983(3), Sn1−C101 2.191(3), Sn2−C100 2.155(3), C100−C101 1.345(5), Sn1−C1 2.162(3), Sn2−C11 2.172(3), Sn1−C17 2.154 (3), Sn2−C53 2.202(3), Sn1−C101−C100 106.7(2), Sn2−C100−C101 114.7(3), C1−Sn1−C17 107.62(1), C11−Sn2−C53 109.41(1), C1−Sn1−Sn2 107.63(9), C11−Sn2−Sn1 107.99(8), C17−Sn1−Sn2 128.97(9), C53−Sn2−Sn1 140.06(9), C101−Sn1−C17 132.89(1), C100−Sn2−C53 108.40(1).

of $^{2}J_{Sn-H}$ and $^{3}J_{Sn-H}$ coupling, giving rise to two sets of ^{119}Sn as well as ^{117}Sn satellites. The proton-coupled ^{119}Sn NMR spectra reveal two doublet signals for compounds **5**−**9** caused by the coupling with the olefinic proton attached to the ring. The existence of two resonances indicates the chemical inequivalency of the two tin atoms. The signals are shifted upfield compared to the respective distannene or bis(stannylene), which is consistent with an increase of the coordination number of the tin atoms from three to four.[40,41] In order to improve the signal-to-noise-ratio, proton-decoupled ^{119}Sn NMR spectra were recorded. These allowed us to observe the expected ^{119}Sn and ^{117}Sn satellites due to coupling between the two tin atoms. The spectroscopic data are summarized in Table 1.

Table 1. ^{119}Sn/^{119}Sn{^{1}H} NMR Spectroscopic Data of 1,2-Distannacyclobut-3-enes 5−10

compound	δ (^{119}Sn) [ppm]	$^{2/3}J_{119Sn-H}$ [Hz]	$^{1}J_{119Sn-119Sn}/^{1}J_{119Sn-117Sn}$ [Hz]	$^{2/3}J_{119Sn-Si}$ [Hz]
5	−40, −125	446/127	4624/4419	
6	56, −88	578/193	2488/2389	166/317
7	−44, −118	442/126	4578/4373	
8	−10, −92	490/140	7037/6724	
9	4, −66	547/139	6463/6188	
10	50, −84	575/240	2463/2356	168/315

Reversibility. The first observation of the reversibility of some of these cycloadditions was made when a light yellow sample of pure Ar^{Me}AnapTMS **6** in C_6D_6 solution turned slightly green after 1 h at room temperature. After several hours the solution was intense green. In order to shed light into that observation we conducted ^{1}H and ^{119}Sn NMR experiments. The ^{1}H NMR spectrum of the pure compound **6** clearly shows a singlet signal at −0.22 ppm, which can be assigned to the methyl groups of the trimethylsilyl substituent attached to the four-membered ring. This signal exhibits satellite signals due to $^{2}J_{Si-H}$ and $^{4}J_{Sn-H}$ coupling ($^{2}J_{Si-H}$ = 6.6 Hz, $^{4}J_{117Sn-H}$ = 113.3 Hz, $^{4}J_{119Sn-H}$ = 118.9 Hz). In addition, the spectrum of the intense green solution, obtained from pure Ar^{Me}AnapTMS **6** after several hours in a sealed J. Young NMR tube, shows a second singlet signal at 0.20 ppm with silicon and ^{13}C satellite signals. This signal can be assigned to the methyl groups of free trimethylsilylacetylene ($^{2}J_{Si-H}$ = 7.1 Hz, $^{1}J_{13C-H}$ = 120.1 Hz). Furthermore, the ^{119}Sn NMR spectrum exhibits, in addition to the two resonances of compound **6** at 56 and −88 ppm, one signal at 375 ppm which can be assigned to distannene **1**.

Ar^{Me}AnapPh **5** shows similar behavior, though the color change to light green was visible only after 1 day. Again, the ^{119}Sn NMR spectrum reveals the presence of distannene **1** besides Ar^{Me}AnapPh **5**. However, the sample of Ar^{Me}AnapPh **5** only changes to pale green, indicating that the equilibrium at ambient temperature lies further on the side of the cycloaddition product than in the case of the sample of Ar^{Me}AnapTMS **6**. This is also supported by ^{119}Sn NMR spectroscopy as the relative share of the signal of distannene **1** compared to the signals of Ar^{Me}AnapPh **5** or Ar^{Me}AnapTMS **6** is in the case of Ar^{Me}AnapTMS **6** remarkably higher. In addition, the reaction of bis(stannylene) **4** with phenylacetylene shows a similar behavior. After a few days, the color of a solution of pure Ar^{iPr}XantPh **9** changes from light yellow to orange-brown and ^{1}H and ^{119}Sn NMR spectra show partial reformation of bis(stannylene) **4**. The formation of Ar^{Me}NapPh **7** and Ar^{Me}XantPh **8**, in contrast, does not show any indication of reversibility at room temperature. The thermal stability of both compounds was examined by heating a C_6D_6 solution for several days in a sealed J. Young NMR tube up to 60 °C. No significant change of the ^{1}H NMR spectra was observed.

In order to shed further light into the role of the backbone, distannene **2** was also reacted with an excess of trimethylsilylacetylene. The ^{119}Sn NMR spectrum of the crude reaction mixture reveals two doublet signals at 50 and −84 ppm, indicating the quantitative formation of a similar cycloaddition product as in the case of compounds **5**−**9**. After removing the excessive trimethylsilylacetylene under reduced pressure and dissolving the residue, the ^{119}Sn NMR spectrum shows an additional signal at 396 ppm which can be assigned to distannene **2**, implying the extrusion of acetylene from the cycloadduct. Furthermore, a color change of the sample from light green to intense green was observed, supporting the assumption of reversibility. As distannene **2** shows reversible and irreversible cycloaddition reactions depending on the acetylene, we cannot draw a clear correlation between the backbone of the distannene and the observed reversibility. However, crystallization of Ar^{Me}NapTMS **10** has so far not been successful, and we were not able to prove the reversibility by dissolving crystals of Ar^{Me}NapTMS **10** and monitoring a probable backward reaction.

For determination of the thermodynamic parameters of the equilibrium reaction a van't Hoff analysis of variable-temperature ^{1}H NMR spectroscopy of the dissociation reaction of Ar^{Me}AnapTMS **6** was performed and afforded a change in enthalpy of dissociation (ΔH_{diss}) of 71.6 kJ·mol^{-1} and a change in entropy (ΔS_{diss}) of 190.5 J·K^{-1}·mol^{-1}. Using the Gibbs−Helmholtz equation, ΔG_{diss} at 298.15 K = 14.8 kJ·mol^{-1}, describing the dissociation reaction as an endergonic process. Unfortunately, a van't Hoff analysis of the reactions with phenylacetylene was not possible due to overlapping signals in ^{1}H NMR spectra. In addition to the experimental results, the

DOI: 10.1021/acs.inorgchem.5b00896
Inorg. Chem. 2015, 54, 6020−6027

enthalpies of dissociation (ΔH_{diss}) at 298.15 K of distannacyclobutenes **5**−**7** were computed by DFT calculations.[42] The computed value of the enthalpy of dissociation of Ar^{Me}AnapTMS **6**, ΔH_{diss} = 70.9 kJ·mol^{-1}, is in surprisingly good accordance with the experimental results, taking into account that solvation effects are not considered. Changing the substituent on the acetylene from trimethylsilyl to phenyl results in a more endothermic dissociation reaction. This is indicated by the calculated dissociation enthalpy of ΔH_{diss} = 96.0 kJ·mol^{-1} for Ar^{Me}AnapPh **5**. Furthermore, the variation of the backbone from acenaphthene to naphthalene likewise results in a higher dissociation enthalpy of ΔH_{diss} = 99.0 kJ·mol^{-1}.

The insolubility of Ar^{Me}AnapPh **5** and Ar^{Me}AnapTMS **6** in *n*-hexane as well as the use of an excess of the acetylenes seem to be the driving forces for the formation of the four-membered cycles. The removal of the excessive acetylene and the change of solvent enables the backward reaction. A possible explanation for the existence of an equilibrium reaction could be ring strain in the four-membered cycles. The reaction of distannene **2** with phenylacetylene does not show reversibility at room temperature, which implies a higher activation energy barrier preventing the backward reaction. Furthermore, the substituent on the acetylene seems to have an influence on the location of the equilibrium. Using the sterically demanding trimethylsilyl substituent on the acetylene compared to the less demanding phenyl substituent in the reaction of distannene **1**, the equilibrium is shifted further to the side of the starting material.

CONCLUSION

Cyclic distannenes with varying backbones and a bis(stannylene) with a xanthene backbone react with phenylacetylene or trimethylsilylacetylene to give products of cycloaddition reactions. With no obvious correlation to the molecular structures these ring formation reactions are at ambient temperature reversible in four cases and irreversible in two cases. On the basis of a van't Hoff analysis and in comparison to quantum chemical calculations the dissociation enthalpy of a distannacyclobutene was determined.

EXPERIMENTAL SECTION

General Procedures. All manipulations were carried out under an argon atmosphere using standard Schlenk techniques or an MBraun Glovebox. Diethyl ether and benzene were distilled from sodium/benzophenone, while *n*-hexane was obtained from an MBraun solvent purification system. Benzene-d_6 was also distilled from sodium. In addition, all solvents were repeatedly degassed by several freeze−pump−thaw cycles and stored in a glovebox. Distannenes **2**/**3** and bis(stannylene) **4** as well as $[2,6\text{-}Mes_2C_6H_3SnCl]_2$ were prepared according to published procedures.[29−31] All other compounds were purchased commercially (Aldrich) and used without further purification. Elemental analysis was performed by the Institut für Anorganische Chemie, Universität Tübingen, using a Vario MICRO EL analyzer. NMR spectra were recorded on a Bruker DRX-250 NMR spectrometer (^{1}H 250.13 MHz, ^{13}C 62.90 MHz, ^{119}Sn 93.28 MHz) equipped with a 5 mm ATM probe head, a Bruker AvanceII+400 NMR spectrometer (^{1}H 400.13 MHz, ^{13}C 100.61 MHz) equipped with a 5 mm QNP (quad nucleus probe) head, or a Bruker AvanceII +500 NMR-spectrometer (^{1}H 500.13 MHz, ^{13}C 125.76 MHz, ^{119}Sn 186.50 MHz) equipped with a 5 mm ATM or a 5 mm TBO probe head and a setup for variable temperature. The chemical shifts are reported in δ values in ppm relative to external $SiMe_4$ (^{1}H, ^{13}C) or $SnMe_4$ (^{119}Sn) using the chemical shift of the solvent ^{2}H resonance frequency and Ξ = 25.145020% for ^{13}C and 37.290632% for ^{119}Sn.[43] The multiplicity of the signals is indicated as s = singlet, d = doublet, t = triplet, and m = multiplet or unresolved. For the assignment of proton and carbon signals detailed analysis of ^{1}H, ^{13}C{^{1}H}, ^{1}H−^{1}H COSY, ^{1}H−^{13}C HSQC, ^{1}H−^{13}C HMBC, and ^{13}C{^{1}H} DEPT 135 spectra was done.

*$[(2,6\text{-}Mes_2)C_6H_3Sn]_2C_{12}H_8$ (**1**).* A solution of 5,6-dibromoacenaphthene (0.2 g, 0.64 mmol, 1 equiv) in Et_2O (5 mL) was cooled to −40 °C. While stirring, a 1.6 M *n*-BuLi solution in *n*-hexane (0.80 mL, 1.28 mmol, 2 equiv) was added dropwise at ambient temperature. The resulting yellow solution was then stirred for 10 min. The solvent and *n*-butyl bromide were removed under reduced pressure (10^{-3} mbar, 1 h). The slightly yellow residue was redissolved in Et_2O (3 mL) and cooled to −40 °C. While stirring, the solution was added dropwise to a cooled solution (−40 °C) of $[2,6\text{-}Mes_2C_6H_3SnCl]_2$ (0.49 g, 0.64 mmol, 1 equiv) in Et_2O (40 mL). The resulting intense green mixture was stirred overnight at ambient temperature. The solvent was removed under reduced pressure, and the residue was extracted into *n*-hexane (60 mL). The *n*-hexane extracts were filtered through Celite, and the filtrate was reduced to incipient crystallization (ca. 20 mL). The mixture was allowed to crystallize at −40 °C for several days. Filtration of the cool supernatant solution yielded the intense green product **1**. The filtrate was further concentrated, and a second crop of the product could be obtained by repeated crystallization yielding compound **1** as a green crystalline solid. Combined yield: 0.34 g, 0.33 mmol, 52%. ^{1}H (C_6D_6, 500.13 MHz): δ (ppm) 2.04 (s, 12H, CH_3-mes), 2.15 (s, 12H, CH_3-mes), 2.42 (s, 12H, CH_3-mes), 3.07 (s, 4H, $CH_2-C_{12}H_8$), 6.42 (s, 4H, *m*-CH-mes), 6.62 (s, 4H, *m*-CH-mes), 7.17 (d, $^3J_{H-H}$ = 7.6 Hz, 4H, *m*-C_6H_3), 7.28 (d, $^3J_{H-H}$ = 6.7 Hz, 2H, CH−$C_{12}H_8$), 7.39 (t, $^3J_{H-H}$ = 7.6 Hz, 2H, *p*-C_6H_3), 8.09 (d, $^3J_{H-H}$ = 7.2 Hz, 2H, CH−$C_{12}H_8$). ^{13}C{^{1}H} (C_6D_6, 125.76 MHz): δ (ppm) 20.7, 21.3, 21.4 (CH_3-mes), 30.0 ($CH_2-C_{12}H_8$), 118.5 (CH−$C_{12}H_8$), 127.6−128.1 ($CH_2-C_{12}H_8$/*m*-C_6H_3 superimposed by solvent signal), 128.7 (*m*-CH-mes), 128.9 (*p*-C_6H_3), 129.01 (*m*-CH-mes), 135.2 (CH−$C_{12}H_8$), 136.0 (*o*-C-mes), 136.3 (*o*-C-mes), 137.1 (*p*-C-mes), 137.6 (C−$C_{12}H_8$), 140.7 (C−$C_{12}H_8$, *ipso*-C-mes), 146.3 (C−$C_{12}H_8$), 149.2 (*o*-C_6H_3), 161.8 (*ipso*-C_6H_3), 173.4 (*ipso*-C−$C_{12}H_8$). ^{119}Sn{^{1}H} (C_6D_6, 186.50 MHz): δ (ppm) 376 (s, $^1J_{119Sn-117Sn}$ = 9478 ± 30 Hz). Anal. Calcd for $C_{60}H_{58}Sn_2$: C, 70.89; H, 5.75. Found: C, 69.58; H, 4.50.

*$[(2,6\text{-}Mes_2)C_6H_3Sn]_2C_{12}H_8C_2HPh$ (**5**).* Distannene **1** (50.0 mg, 49.2 μmol, 1 equiv) was dissolved in *n*-hexane (6 mL) and stirred with an excess of phenylacetylene (ca. 0.05 mL) at ambient temperature for several days until an off-white precipitate was formed. The precipitate was isolated by filtration and dried under reduced pressure. A concentrated solution in benzene was allowed to crystallize at ambient temperature for a few days and yielded the pure product as slightly yellow crystals (37.3 mg, 33.3 μmol, 68%). ^{1}H (C_6D_6, 400.13 MHz): δ (ppm) 1.81, 2.19, 2.22, 2.37, 2.46, 2.50 (s, 6H, CH_3-mes), 3.09 (m, 4H, $CH_2-C_{12}H_8$), 5.73 (s, $^2J_{117Sn-H}$ = 406.9 Hz, $^2J_{119Sn-H}$ = 426.6 Hz, $^3J_{117Sn-H}$ = 125.0 Hz, $^3J_{119Sn-H}$ = 130.7 Hz, 1H, CH−HC_2Ph), 6.18, 6.65 (s, 2H, *m*-CH-mes), 6.84−6.89 (m, 3H, *o*-CH−C_6H_5, CH−$C_{12}H_8$), 6.94−6.98 (m, 5H, *m*-CH-mes, CH−$C_{12}H_8$), 7.02−7.05 (m, 3H, *m*-CH−C_6H_5, *p*-CH−C_6H_5), 7.15−7.19 (m, 5H, *m*-C_6H_3, CH−$C_{12}H_8$), 7.33, 7.43 (t, $^3J_{H-H}$ = 7.5 Hz, 1H, *p*-C_6H_3), 7.74 (d + 2 dd, $^3J_{H-H}$ = 6.6 Hz, $^{3/4}J_{117Sn-H}$ = 31.7 Hz, $^{3/4}J_{119Sn-H}$ = 45.2 Hz, 1H, CH−$C_{12}H_8$). ^{13}C{^{1}H} (C_6D_6, 100.60 MHz): δ (ppm) 20.9, 21.0, 21.3, 21.5, 21.7, 21.8 (CH_3-mes), 29.6, 29.7 ($CH_2-C_{12}H_8$), 117.5 (CH−$C_{12}H_8$), 118.3 (CH−$C_{12}H_8$/*o*-CH−C_6H_5), 125.3 (CH−$C_{12}H_8$), 126.1(CH−$C_{12}H_8$/*o*-CH−C_6H_5), 127.0 (*m*-CH−C_6H_5, *p*-CH−C_6H_5), 128.3 (*o*-C-mes/*p*-C-mes), 128.5 (*m*-CH-mes), 128.6, 128.7 (*m*-CH-mes/CH−$C_{12}H_8$/*m*-C_6H_3), 129.0 (*m*-CH-mes), 129.8 (*m*-C_6H_3/*p*-C_6H_3/CH−$C_{12}H_8$),134.9 (*m*-CH−C_6H_5, *p*-CH−C_6H_5), 135.4, 135.5 (*o*-C-mes/*ipso*-C-mes), 135.9 (CH−$C_{12}H_8$), 136.0, 136.2,136.3, 136.4, 136.6 (*o*-C-mes/*ipso*-C-mes),139.1, 139.2 (*m*-CH−C_6H_5/*p*-CH−C_6H_5/C−$C_{12}H_8$), 140.4, 141.3 (*o*-C-mes/*p*-C-mes), 141.7 (C−$C_{12}H_8$), 143.1 (quart. C_{Aryl}), 143.5 (C−$C_{12}H_8$), 144.0 (*ipso*-C−C_6H_3/*ipso*-C−C_6H_5/*ipso*-C−$C_{12}H_8$/C−$C_{12}H_8$), 145.0 (*ipso*-C−C_6H_5/*o*-CH−C_6H_5), 145.8, 145.9 (*m*-CH−C_6H_5/*p*-CH−C_6H_5/C−$C_{12}H_8$), 146.7 (C−$C_{12}H_8$/*ipso*-C-mes), 147.2 (*ipso*-C−C_6H_3/*ipso*-C−C_6H_5/*ipso*-C−$C_{12}H_8$), 149.8(*o*-C_6H_3, according to HMBC), 150.7 (*o*-C_6H_3), 154.4 (CH−HC_2Ph),

DOI: 10.1021/acs.inorgchem.5b00896
Inorg. Chem. 2015, 54, 6020−6027

171.6 (C−HC_2Ph). ^{119}Sn (C_6D_6, 93.28 MHz): δ (ppm) −40 (d, $^{2/3}J_{Sn-H}$ = 446 Hz), −125 (d, $^{2/3}J_{Sn-H}$ = 127 Hz). ^{119}Sn{^{1}H} (C_6D_6, 93.28 MHz): δ (ppm) −40 (s, $^1J_{119Sn-119Sn}$ = 4624 ± 30 Hz, $^1J_{119Sn-117Sn}$ = 4419 ± 30 Hz), −125 (s, $^1J_{119Sn-119Sn}$ = 4624 ± 30 Hz, $^1J_{119Sn-117Sn}$ = 4419 ± 30 Hz). Anal. Calcd for $C_{68}H_{64}Sn_2{\cdot}C_6D_6$: C, 74.27; H, 5.90. Found: C, 74.15; H, 5.52.

*[(2,6-Mes$_2$)C$_6$H$_3$Sn]$_2$C$_{12}$H$_8$C$_2$HSiMe$_3$ (**6**).* Following a similar protocol as for the preparation of compound **5**, product **6** was obtained as yellow-green crystals. The crystals were washed with 0.5 mL of cold *n*-hexane in order to get rid of small amounts of distannene **1**, which was formed because of the reversibility of the reaction at ambient temperature, resulting in slightly yellow crystals (30.5 mg, 27.3 μmol, 56%). ^{1}H (C_6D_6, 500.13 MHz): δ (ppm) −0.22 (s, $^3J_{Si-H}$ = 6.62 Hz, J_{Sn-H} = 118.90 Hz, 9H, Si(CH_3)$_3$), 2.17−2.46 (m, 36H, CH_3-mes), 3.05 (m, 4H, $CH_2-C_{12}H_8$), 6.69 (d, 1H, $^3J_{H-H}$ = 6.7 Hz, CH−$C_{12}H_8$), 6.77 (s, 2H, *m*-CH-mes), 6.87 (m, 4H, CH−$C_{12}H_8$, *m*-CH-mes, CH−$HC_2Si(CH_3)_3$), 7.01 (br s, 2H, *m*-CH-mes), 7.13 (d, $^3J_{H-H}$ = 7.5 Hz, 3H, *m*-C_6H_3, CH−$C_{12}H_8$), 7.18 (d, $^3J_{H-H}$ = 7.6 Hz, 2H, *m*-C_6H_3), 7.26 (s, 2H, *m*-CH-mes (superimposed by solvent signal)), 7.31 (t, $^3J_{H-H}$ = 7.5 Hz, 1H, *p*-C_6H_3), 7.43 (t, $^3J_{H-H}$ = 7.6 Hz, 1H, *p*-C_6H_3). ^{13}C{^{1}H} (C_6D_6, 125.76 MHz): δ (ppm) 0.7 (Si(CH_3)$_3$), 20.9, 21.7, 21.8 (CH_3-mes), 29.7 ($CH_2-C_{12}H_8$), 117.7, 118.2 (CH−$C_{12}H_8$), 127.6−128.0 (*m*-CH-mes superimposed by solvent signal), 128.3 (*m*-C_6H_3), 128.5, 128.7 (3 × *m*-CH-mes), 128,8 (*m*-C_6H_3), 129.5, 129.8 (*p*-C_6H_3), 134.1, 136.0 (CH−$C_{12}H_8$), 136.1, 136.3, 136.5, 136.6, 137.8 ($C_{Aryl,\ quart}$), 139.0($C_{quart}-C_{12}H_8$/*ipso*-C-mes), 141.2 (*ipso*-C-mes), 143.2, 144.9 ($C_{quart}-C_{12}H_8$), 145.3 ($C_{quart}-C_{12}H_8$/*ipso*-C-mes), 146.6 ($C_{quart}-C_{12}H_8$), 146.7 (*ipso*-C-mes), 148.1 ($C_{quart}-C_{12}H_8$), 150.1 (*o*-C_6H_3), 169.5 (CH−$HC_2Si(CH_3)_3$), 176.7 (C−$HC_2Si(CH_3)_3$)). ^{119}Sn (C_6D_6, 93.28 MHz): δ (ppm) 56 (d, $^{2/3}J_{Sn-H}$ = 578 Hz), −87 (d, $^{2/3}J_{Sn-H}$ = 193 Hz). ^{119}Sn{^{1}H} (C_6D_6, 93.28 MHz): δ (ppm) 56 (s + 3 d, $^{2/3}J_{Sn-Si}$ = 166 Hz, $^1J_{119Sn-119Sn}$ = 2466 ± 30 Hz, $^1J_{119Sn-117Sn}$ = 2353 ± 30 Hz), −87 (s + 3 d, $^{2/3}J_{Sn-Si}$ = 317 Hz, $^1J_{119Sn-119Sn}$ = 2488 ± 30 Hz, $^1J_{119Sn-117Sn}$ = 2389 ± 30 Hz). ^{29}Si DEPT45 (C_6D_6, 49.69 MHz): −7.1 (s). Anal. Calcd for $C_{65}H_{67}SiSn_2$: C, 70.10; H, 6.06. Found: C, 70.21; H, 5.83.

*[(2,6-Mes$_2$)C$_6$H$_3$Sn]$_2$C$_{10}$H$_6$C$_2$HPh (**7**).* Distannene **2** (50.0 mg, 50.5 μmol, 1 equiv) was dissolved in *n*-hexane (6 mL) and stirred with an excess of phenylacetylene (ca. 0.05 mL) at ambient temperature for several days until a color change to red-orange was completed. All volatiles were removed under reduced pressure. A concentrated solution in *n*-hexane was allowed to crystallize at ambient temperature for a few days and yielded the pure product as yellow crystals (21.5 mg, 19.7 μmol, 39%). ^{1}H (C_6D_6, 400.13 MHz): δ (ppm) 1.78, 2.15, 2.22, 2.31, 2.43, 2.47 (s, 6H, CH_3-mes), 5.64 (s, $J_{117Sn-H}$ = 124.2 Hz, $J_{119Sn-H}$ = 129.2 Hz, $J_{117Sn-H}$ = 405.5 Hz, $J_{119Sn-H}$ = 424.5 Hz, 1H, CH−HC_2Ph), 6.12, 6.61 (s, 2H, *m*-CH-mes), 6.86−6.90 (m, 4H, *m*-CH-mes, CH−C_6H_5), 6.95−6.99 (m, 5H, *m*-CH-mes, CH−$C_{10}H_6$, *m*-C_6H_3), 7.03−7.04 (m, 2H, CH−C_6H_5), 7.16 (m, 4H, CH−C_6H_5, CH−$C_{10}H_6$, *m*-C_6H_3), 7.30 (m, 1H, CH−$C_{10}H_6$), 7.33 (m, 1H, *p*-C_6H_3), 7.42 (t, $^3J_{H-H}$ = 7.6, 1H, *p*-C_6H_3), 7.46, 7.63 (dd, $^3J_{H-H}$ = 8.2 Hz, $^3J_{H-H}$ = 1.4, 1H, CH−$C_{10}H_6$), 7.73 (dd, $^3J_{H-H}$ = 6.6, $^3J_{H-H}$ = 1.4, 1H, CH−$C_{10}H_6$). ^{13}C{^{1}H} (C_6D_6, 100.60 MHz): δ (ppm) 20.7, 20.9 (2 × CH_3-mes), 21.3, 21.6, 21.8 (CH_3-mes), 123.1 (CH−$C_{10}H_6$), 124.1 (*m*-C_6H_3), 125.3 (CH−$C_{10}H_6$/*m*-CH-mes), 126.1 (CH−C_6H_5), 127.0 (CH−C_6H_5), 127.6−128.0 (CH−$C_{10}H_6$), 128.7−128.8 (*m*-CH-mes, CH−$C_{10}H_6$, CH−C_6H_3, CH−C_6H_5), 129.1 (*m*-CH-mes), 129.7 (CH−$C_{10}H_6$), 129.9 (2 × *p*-C_6H_3), 130.5 (quart. C_{Aryl}), 134.0 (CH−$C_{10}H_6$/CH−C_6H_3/*m*-CH-mes), 134.7 (quart. C_{Aryl}), 135.0 (CH−$C_{10}H_6$), 135.3, 135.5, 135.8, 136.0, 136.2, 136.3, 136.5, 136.6, 139.2, 140.2, 141.2, 141.7, 142.8, 144.1, 144.4, 147.2, 150.7, 151.5 ($C_{Aryl,quart}$), 154.1 (CH−HC_2Ph), 172.1 ($C_{Aryl,quart}$). ^{119}Sn (C_6D_6, 93.28 MHz): δ (ppm) −44 (d, $^{2/3}J_{Sn-H}$ = 415.1 Hz), −118 (d, $^{2/3}J_{Sn-H}$ = 126.3 Hz). ^{119}Sn{^{1}H} (C_6D_6, 93.28 MHz): δ (ppm) −44 (s + 2 d, $^1J_{119Sn-119Sn}$ = 4578 ± 30 Hz, $^1J_{119Sn-117Sn}$ = 4373 ± 30 Hz), −118 (s + 2 d, $^1J_{119Sn-119Sn}$ = 4578 ± 30 Hz, $^1J_{119Sn-117Sn}$ = 4373 ± 30 Hz). Anal. Calcd for $C_{66}H_{62}Sn_2$: C, 72.55; H, 5.72. Found: C, 72.40; H, 5.17.

*[(2,6-Mes$_2$)C$_6$H$_3$Sn]$_2$C$_{15}$H$_{12}$OC$_2$HPh (**8**).* Distannene **3** (100 mg, 93 μmol, 1 equiv) and phenylacetylene (10 mg, 98 μmol, 1.05 equiv) were stirred in *n*-hexane (10 mL) at ambient temperature overnight. The reaction mixture turned colorless, and colorless product **8** precipitated. The precipitate was isolated by filtration and dried under reduced pressure. The filtrate was placed in a freezer at −40 °C, and cold filtration yielded a second crop of product **8** (70 mg, 59.5 μmol 64%). Few single crystals were obtained from a concentrated solution in *n*-hexane after crystallization for a few days at ambient temperature. ^{1}H (C_6D_6, 500.13 MHz): δ (ppm) 1.32 (s, 3H, CH_3-xan), 1.39 (s, 3H, CH_3-xan), 1.92 (br s, 3H, CH_3-mes), 1.98 (br s, 3H, CH_3-mes), 2.01 (s, 3H, CH_3-mes), 2.04 (br s, 3H, CH_3-mes), 2.15−2.25 (br resonances, 6H, CH_3-mes), 2.19 (s, 3H, CH_3-mes), 2.25 (s, 3H, CH_3-mes), 2.29 (s, 3H, CH_3-mes), 2.33 (s, 3H, CH_3-mes), 2.35 (s, 3H, CH_3-mes), 2.40 (br s, 3H, CH_3-mes), 5.94 (br s, 1H, *m*-CH-mes), 6.33 (br s, 1H, *m*-CH-mes), 6.38 (s + 4 d, $J_{119Sn-H}$ = 487 Hz, $J_{117Sn-H}$ = 464 Hz, $J_{119Sn-H}$ = 141 Hz, $J_{117Sn-H}$ = 135 Hz, CH−HC_2Ph), 6.63−6.64 (m, 3H, 2× *o*-CH−C_6H_5, CH−Ar), 6.68 (s, 1H, CH−Ar), 6.70 (s, 1H, CH−Ar), 6.71 (s, 1H, CH−Ar), 6.74−6.77 (m, 1H, CH-xan), 6.79−6.80 (m, 1H, CH-xan), 6.87−7.00 (m, 8H, 2 × CH-xan, 2 × *m*-CH−C_6H_5, *p*-CH−C_6H_5, 3 × CH-Ar), 7.05 (s, 1H, CH−Ar), 7.06−7.08 (m, 1H, CH−Ar), 7.10 (br s, 1H, CH−Ar), 7.23−7.28 (m, 3H, CH-xan, 2 × CH−Ar), 7.34 (dd + tin satellites, $^3J_{H-H}$ = 7.2 Hz, $^4J_{H-H}$ = 1.3 Hz, $J_{119/117Sn-H}$ = 28 Hz, CH-xan). ^{13}C{^{1}H} (C_6D_6, 125.76 MHz): δ (ppm) 21.3, 21.4 (CH_3-mes), 21.4−21.6 (*br*, CH_3-mes), 21.7, 21.8, 21.9 (CH_3-mes), 22.2 (multiple resonances, CH_3-mes), 23.0 (br, CH_3-mes), 23.2 (2s, CH_3-xan and CH_3-mes), 29.4 (s, 1C, CH_3-xan), 37.6 (C(CH_3)$_2$-xan), 123.1, 123.2, 123.3, 124.5 (CH-xan), 125.9 (*p*-CH−C_6H_5), 126.7 (2 × *o*-CH−C_6H_5), 126.8 (2 × *m*-CH−C_6H_5), 128.6, 128.8, 128.9, 129.0, 129.3 (C_{Aryl}), 128.8−129.4 (elevated underground probably arising from br C_{Aryl} resonances), 129.6, 129.8, 130.0 (C_{Aryl}), 132.9 (CH-xan), 134.2 (C-xan), 134.7 (CH-xan), 135.5 (br), 135.8 (C-xan and C_{Aryl}), 135.9, 135.9 (C_{Aryl}), 136.5 (C-xan), 136.5, 136.5, 136.6, 137.1, 137.4 (C_{Aryl}), 140.7 (br), 141.0 (br), 141.5, 142.1 (C_{Aryl}), 147.0 (2 s, C−C_6H_5 and C_{Aryl}), 147.2 (C_{Aryl}), 149.2 (br, C_{Aryl}), 150.3 (C_{Aryl}), 158.6, 160.3 (C-xan), 161.1 (CH−HC_2Ph), 176.6 (C−HC_2Ph). ^{119}Sn (C_6D_6, 93.28 MHz): δ (ppm) −10 (d, $^{2/3}J_{Sn-H}$ = 490 Hz), −92 (d, $^{2/3}J_{Sn-H}$ = 140 Hz). ^{119}Sn{^{1}H} (C_6D_6, 186.50 MHz): δ (ppm) −10 (s + 2d, $^1J_{119Sn-119Sn}$ = 7037 ± 30 Hz, $^1J_{119Sn-117Sn}$ = 6724 ± 30 Hz), −92 (s + 2d, $^1J_{119Sn-119Sn}$ = 7037 ± 30 Hz, $^1J_{119Sn-117Sn}$ = 6724 ± 30 Hz). Anal. Calcd for $C_{71}H_{68}OSn_2$: C, 72.59; H, 5.83. Found: C, 72.66; H, 5.66.

*[(2,6-Trip$_2$)C$_6$H$_3$Sn]$_2$C$_{15}$H$_{12}$OC$_2$HPh (**9**).* Bis(stannylene) **4** (100 mg, 36 μmol, 1 equiv) was dissolved in *n*-hexane (5 mL) and stirred with an excess of phenylacetylene (10 mg, 98 μmol, 1.72 equiv) at ambient temperature overnight. A color change from red-brown to light yellow was observed. The solvent was removed under reduced pressure. A concentrated solution in Et_2O was allowed to crystallize at −40 °C to yield the product as yellow crystals (46.1 mg, 30.5 μmol, 43%). ^{1}H (C_6D_6, 400.13 MHz): δ (ppm) 0.93−1.43 (multiple resonances, 78H, CH_3-iPr and CH_3-xan), 2.59 (m, 3H, CH-iPr), 2.76 (sept, 1H, CH-iPr), 2.90 (m, 2H, CH-iPr), 3.12 (sept, 1H, CH-iPr), 3.33 (m, 3H, CH-iPr), 3.46 (sept, 1H, CH-iPr), 3.71 (sept, 1H, CH-iPr), 6.44−6.49 (multiple resonances, 3H, CH−Ar), 6.53−6.56, m, 1H, CH−Ar), 6.71 (s + 2 d, $J_{119Sn-H}$ = 512 Hz, $J_{117Sn-H}$ = 492 Hz, CH−HC_2Ph), 6.73−7.25 (multiple resonances, CH−Ar), 7.45(dd, 1H, CH−Ar), 7.63 (dd, 1H, CH−Ar). ^{13}C{^{1}H} (toluene-d_8, 100.62 MHz): δ (ppm) 23.7, 24.2, 24.4, 24.5, 24.6, 25.1, 25.2, 25.4, 25.7, 25.9, 26.1, 26.4, 26.5, 26.6, 26.7, 26.9, 27.3, 27.6, 27.9, 30.4, 30.5, 30.7, 30.8, 31.0 (2 ×), 31.3, 31.4, 31.6, 32.3, 34.1, 34.6 (2×), 34.7, 36.9, 47.3, 56.7, 77.7, 83.9, 120.0, 120.7 (2×), 120.9, 121.3, 121.4, 121.6, 122.1, 122.9, 123.0, 123.2, 123.3, 123.7, 124.7, 125.8, 126.2, 127.1, 127.3, 127.5, 128.1, 128.3, 128.4 (2×), 128.7, 130.5, 132.3, 132.4, 132.5, 132.7, 132.9, 134.0, 134.1, 135.7, 137.1, 137.7, 137.9, 138.6 (2×), 140.3, 141.7, 145.7, 145.8, 146.0, 146.1, 147.1, 147.2, 147.4, 147.6, 147.8 (2×), 148.0, 148.2, 148.3, 148.6, 148.7, 148.9 (2×), 149.0. ^{119}Sn (C_6D_6, 93.28 MHz): δ (ppm) −66 (d, $^{2/3}J_{Sn-H}$ = 139 Hz), 4 (d, $^{2/3}J_{Sn-H}$ = 547 Hz). ^{119}Sn{^{1}H} (C_6D_6, 93.27 MHz): δ(ppm) −66 (s + 2 d, $^1J_{119Sn-119Sn}$ = 6463 Hz, $^1J_{119Sn-117Sn}$ = 6188 Hz), 4 (s + 2 d, $^1J_{119Sn-119Sn}$ = 6463 Hz, $^1J_{119Sn-117Sn}$ = 6188 Hz). Anal. Calcd for $C_{95}H_{116}OSn_2$: C, 75.50; H, 7.74. Found: C, 75.51; H, 7.40.

DOI: 10.1021/acs.inorgchem.5b00896
Inorg. Chem. 2015, 54, 6020−6027

*[(2,6-Mes_2)$C_6H_3Sn]_2C_{10}H_6C_2HSiMe_3$ (**10**).* In a J. Young NMR tube distannene **2** (30.2 mg, 30.5 μmol, 1 equiv) was dissolved in C_6D_6 (0.5 mL), and an excess of trimethylsilylacetylene (ca. 0.05 mL) was added at ambient temperature. After 2 days the intense green color of the solution got lighter. The ^{119}Sn NMR spectrum reveals two doublet signals at 50 and −84 ppm, indicating quantitative formation of a similar cycloaddition product as in the case of compounds **5**−**9**. After removing the excess acetylene from the crude reaction mixture in vacuo and dissolving the residue in C_6D_6, the ^{119}Sn NMR spectrum shows an additional signal at 396 ppm which is assigned to distannene **2**. Furthermore, a color change from light green to intense green was observed. Reasonable interpretation of the ^{1}H or ^{13}C NMR spectrum was not possible due to the reversibility of the reaction. Furthermore, no crystals could be obtained so far, which is probably also caused by the reversibility. The spectral data are shown in the Supporting Information. ^{119}Sn (C_6D_6, 93.28 MHz): δ (ppm) 50 (d, $^{2/3}J_{Sn-H}$ = 575 Hz), −84 (d, $^{2/3}J_{Sn-H}$ = 240 Hz). ^{119}Sn{^{1}H} (C_6D_6, 93.28 MHz): δ (ppm) 50 (s + 3 d, $^{2/3}J_{Sn-Si}$ = 168 Hz, $^1J_{119Sn-119Sn}$ = 2466 ± 30 Hz, $^1J_{119Sn-117Sn}$ = 2358 ± 30 Hz), −84 (s + 3 d, $^{2/3}J_{Sn-Si}$ = 315 Hz, $^1J_{119Sn-119Sn}$ = 2460 ± 30 Hz, $^1J_{119Sn-117Sn}$ = 2354 ± 30 Hz).

■ ASSOCIATED CONTENT

Supporting Information

Details on X-ray data, NMR spectra, van't Hoff analysis, and DFT calculations. The Supporting Information is available free of charge on the ACS Publications website at DOI: 10.1021/acs.inorgchem.5b00896.

■ AUTHOR INFORMATION

Corresponding Author

*E-mail: lars.wesemann@uni-tuebingen.de.

Notes

The authors declare no competing financial interest.

■ ACKNOWLEDGMENTS

We thank the Landesgraduiertenförderung BW (fellowship J.S.) and the Fond der Chemischen Industrie (fellowship J.H.) for financial support and the bwGrid cluster Tübingen for provision of computational resources. Kristina Strohmaier and Dr. Klaus Eichele are acknowledged for technical support.

■ REFERENCES

(1) Davidson, P. J.; Harris, D. H.; Lappert, M. F. *J. Chem. Soc., Dalton Trans.* **1976**, 2268−2274.
(2) Goldberg, D. E.; Harris, D. H.; Lappert, M. F.; Thomas, K. M. *J. Chem. Soc., Chem. Commun.* **1976**, 261−262.
(3) Driess, M.; Grützmacher, H. *Angew. Chem., Int. Ed. Engl.* **1996**, *35*, 828−856.
(4) Power, P. P. *J. Chem. Soc., Dalton Trans.* **1998**, 2939−2951.
(5) Power, P. P. *Chem. Rev.* **1999**, *99*, 3463−3504.
(6) Kira, M.; Iwamoto, T. *Adv. Organomet. Chem.* **2006**, *54*, 73−148.
(7) Wang, Y.; Robinson, G. H. *Chem. Commun.* **2009**, 5201−5213.
(8) Fischer, R. C.; Power, P. P. *Chem. Rev.* **2010**, *110*, 3877−3923.
(9) Okazaki, R.; West, R. *Adv. Organomet. Chem.* **1996**, *39*, 231−273.
(10) Weidenbruch, M. In *The Chemistry of Organic Silicon Compounds*; Rappoport, Z., Apeloig, Y., Eds.; John Wiley & Sons Ltd.: Chichester, UK, 2001; pp 391−428.
(11) Weidenbruch, M. *Organometallics* **2003**, *22*, 4348−4360.
(12) Nefedov, O. M.; Egorov, M. P.; Gal'minas, A. M.; Kolesnikov, S. P.; Krebs, A.; Berndt, J. *J. Organomet. Chem.* **1986**, *301*, C21−C22.
(13) Batcheller, S. A.; Masamune, S. *Tetrahedron Lett.* **1988**, *29*, 3383−3384.
(14) Ando, W.; Tsumuraya, T. *J. Chem. Soc., Chem. Commun.* **1989**, 770.
(15) Tsumuraya, T.; Kabe, Y.; Ando, W. *J. Organomet. Chem.* **1994**, *482*, 131−138.
(16) Weidenbruch, M.; Hagedorn, A.; Peters, K.; von Schnering, H. G. *Angew. Chem., Int. Ed. Engl.* **1995**, *34*, 1085−1086.
(17) Baines, K. M.; Stibbs, W. G. *Adv. Organomet. Chem.* **1996**, *39*, 275−324.
(18) Escudie, J.; Ranaivonjatovo, H. *Adv. Organomet. Chem.* **1999**, *44*, 113−174.
(19) Tokitoh, N.; Okazaki, R. In *The Chemistry of Organic Germanium, Tin and Lead Compounds*; Rappoport, Z., Ed.; John Wiley & Sons, Ltd.: New York, 2002; pp 843−901.
(20) Hurni, K. L.; Baines, K. M. *Chem. Commun.* **2011**, *47*, 8382−8384.
(21) Davidson, P. J.; Lappert, M. F. *J. Chem. Soc., Chem. Commun.* **1973**, 317a.
(22) Sita, L. R.; Bickerstaff, R. D. *J. Am. Chem. Soc.* **1988**, *110*, 5208−5209.
(23) Krebs, A.; Jacobsen-Bauer, A.; Haupt, E.; Veith, M.; Huch, V. *Angew. Chem.* **1989**, *101*, 640−642.
(24) Sita, L. R.; Kinoshita, I.; Lee, S. P. *Organometallics* **1990**, *9* (5), 1644−1650.
(25) Weidenbruch, M.; Schäfer, A.; Kilian, H.; Pohl, S.; Saak, W.; Marsmann, H. *Chem. Ber.* **1992**, *125*, 563−566.
(26) Lee, V. Y.; Fukawa, T.; Nakamoto, M.; Sekiguchi, A.; Tumanskii, B. L.; Karni, M.; Apeloig, Y. *J. Am. Chem. Soc.* **2006**, *128*, 11643−11651.
(27) Peng, Y.; Ellis, B. D.; Wang, X.; Fettinger, J. C.; Power, P. P. *Science* **2009**, *325*, 1668−1670.
(28) Hardwick, J. A.; Baines, K. M. *Angew. Chem.* **2015**, n/a−n/a.
(29) Henning, J.; Wesemann, L. *Angew. Chem., Int. Ed.* **2012**, *51*, 12869−12873.
(30) Henning, J.; Eichele, K.; Fink, R. F.; Wesemann, L. *Organometallics* **2014**, *33*, 3904−3918.
(31) Simons, R. S.; Pu, L.; Olmstead, M. M.; Power, P. P. *Organometallics* **1997**, *16*, 1920−1925.
(32) Klinkhammer, K. W.; Schwarz, W. *Angew. Chem., Int. Ed. Engl.* **1995**, *34*, 1334−1336.
(33) Weidenbruch, M.; Kilian, H.; Peters, K.; Schnering, H. G. V.; Marsmann, H. *Chem. Ber.* **1995**, *128*, 983−985.
(34) Klinkhammer, K. W.; Fässler, T. F.; Grützmacher, H. *Angew. Chem., Int. Ed.* **1998**, *37*, 124−126.
(35) Stürmann, M.; Saak, W.; Klinkhammer, K. W.; Weidenbruch, M. *Z. Anorg. Allg. Chem.* **1999**, *625*, 1955−1956.
(36) Stanciu, C.; Richards, A. F.; Power, P. P. *J. Am. Chem. Soc.* **2004**, *126*, 4106−4107.
(37) Fukawa, T.; Lee, V. Y.; Nakamoto, M.; Sekiguchi, A. *J. Am. Chem. Soc.* **2004**, *126*, 11758−11759.
(38) Kurzbach, D.; Yao, S.; Hinderberger, D.; Klinkhammer, K. W. *Dalton Trans.* **2010**, *39*, 6449−6459.
(39) Arp, H.; Baumgartner, J.; Marschner, C.; Müller, T. *J. Am. Chem. Soc.* **2011**, *133*, 5632−5635.
(40) Wrackmeyer, B. *Annu. Rep. NMR Spectrosc.* **1985**, *16*, 73−186.
(41) Wrackmeyer, B. *Annu. Rep. NMR Spectrosc.* **1999**, *38*, 203−264.
(42) Geometry optimizations were carried out starting from X-ray structures applying the BP86 functional, the GD3BJ dispersion correction, the def2-TZVP basis set, as well as w06 density fitting on all atoms. For further details on DFT calculations, see the Supporting Information.
(43) Harris, R. K.; Becker, E. D.; Cabral de Menezes, S. M.; Goodfellow, R.; Granger, P. *Pure Appl. Chem.* **2001**, *73*, 1795−1818.

DOI: 10.1021/acs.inorgchem.5b00896
Inorg. Chem. 2015, 54, 6020−6027